

Type of the Paper (Article)

# Finite Element Analysis of Adolescent Mandible Fracture Occurring during Accidents

Jarosław Żmudzki <sup>1,\*</sup>, Karolina Panek <sup>2</sup>, Grzegorz Chladek <sup>1</sup>, Marcin Adamiak <sup>1</sup> and Paul Lipinski <sup>3,\*</sup>

<sup>1</sup> Faculty of Mechanical Engineering, Institute of Engineering Materials and Biomaterials, Silesian University of Technology, ul. Konarskiego 18a, 44-100 Gliwice, Poland; grzegorz.chladek@polsl.pl (G.C.); (M.A.)

<sup>2</sup> Graduate student of materials engineering, Faculty of Mechanical Engineering, Institute of Engineering Materials and Biomaterials, Silesian University of Technology, ul. Konarskiego 18a, 44-100 Gliwice, karolina.panek92@gmail.com

<sup>3</sup> LEM3, Université de Lorraine, Ecole Nationale d'Ingénieurs de Metz, 1 route d'Ars Laquenexy, BP 65820, 57 078 Metz Cedex 03, France

\* Correspondence: jaroslaw.zmudzki@polsl.pl (J.Ż); Tel.: +48-32-237-2907; pawel.lipinski@univ-lorraine.fr (P.L); Tel.: +33 (0)3-72-74-86-46

**Featured Application:** Authors are encouraged to provide a concise description of the specific application or a potential application of the work. This section is not mandatory.

**Abstract:** The paper aims in assessing risks of mandible fractures consequent to impacts or sport accidents. The role of the structural stiffness of mandible, related to disocclusion state, is evaluated through numerical simulations using the finite element method (FEM). It has been assumed that the quasi-static stress field, due to distributed forces developed during accidents, could explain the common types of mandibular fractures. Geometric model of adolescent mandible was built, upon the basis of medical imaging, in CAD software with distinction between cortical layer and inner spongy bone. The finite element model of disoccluded mandible was next created. Mandibular condyles were supposed jammed in the maxillary fossae. The total force of 700 N, simulating an impact on mandible, has been sequentially applied in three distinct areas: centrally, at canine zone and at the mandibular angle. Clinically most frequent fractures of mandible were recognized through the analysis of maximal principal stress and maximal principal strain fields. Mandibular fracture during accidents can be analyzed at satisfactory level using linear quasi-static FE models for designing protections in sport and transport. The proposed approach can be improved by introducing more realistic interactions between condylar processes and fossae.

**Keywords:** mandible fracture, disocclusion state, finite element analysis, critical blow force

## 1. Introduction

Injuries in the stomatognathic system, as a consequence of traffic or sports accidents, attained the status of the main public health problem [1]. Following a literature review the authors find that from 76 to 93% of patients who experienced facial wounds suffered mandibular fractures [2,3]. They are mainly located in the condylar neck, in the symphysis and parasymphysis but also in the body and the mandibular angle [4,5].

Studies of tissues under impact forces are essential for research improving safety solutions [6–12]. There are numerous finite element quasi-static analyses of biomechanics of mandible. They concern the force transmission into temporo-mandibular joint (TMJ) [13–16], TMJ implants and bone fixation plates [17–19], distraction osteogenesis [20,21] as also contact phenomena in dental

restorations [22–24] under occlusal forces [25,26] and intra-oral forces of lips and tongue [27,28]. However, numerical studies on risk of mandibular fractures are rarely presented in the literature, although finite element method has been successfully applied in fracture predictions of such bones like femur and tibia [29]. Realistic simulations of deceleration during accidents allow precise determination of dynamic forces. However, they frequently concern greatly simplified bone structures [6,30–32]. Brain injury was the topic of the works [30–32] but the mandible was represented as a simplified structure with average elastic properties of cortical and cancellous bone tissues. However, skull bone answer is depended on its structure and cortical bone layer thickness [33–36] Force transfer to the skull in case of impact to mandible was conducted by Tuchtan et al. [37] taking into account its cortical and cancellous constituents. But the risk of mandibular fracture was not analyzed in this investigation. Simulation and experimental studies [38] show that prediction of fracture localization is possible based on modal vibrational analysis. However, a free-support condition on sponge and stiffness of alveolar processes without periodontal ligament are not consistent with real mandible behavior. Also in the modeling approach developed in works [39,40] the lack of periodontal tooth resiliency makes impossible the analyses of teeth fracture, for example, in design of protections in sport (mouthguards). This fact affects analysis of the mandibular fractures due to incorrect load transfer into bone tissue surroundings excessively stiff alveolar processes [41]. Resiliency of teeth was considered by Bezerra et al. [42] The authors correlated stress concentration around third molars with a high number of fractures [43]. But stresses in bone reached exaggerated value of 180 MPa due to the assumed extreme level of blow force of 250 kgf. Consequently, tendency to the most common fractures of condylar neck was not detectable. Fractures of adolescent mandible during sports are common, despite lower blow forces involved in regards to muscle strengths and body weight. During blow external forces produce stresses, whose distribution in mandible is sensitive to structural stiffness of alveolar processes. In general, the modeling conditions close to real life are crucial for strength analysis but from the other hand they increase computing costs [44]. In this work special attention was paid to mandibular fracture prediction in teenagers. Indeed, they commonly suffer teeth and jawbone injuries during sport and daily activity [45,46].

The aim of this work was to analysis the risk of fracture of adolescent mandible under forces associated with standard accidents. The problem was treated via the FEM simulations based on quasi-static elastic bone answer to a blow on disoccluded mandible. It has been assumed that the quasi-static stress field, due to distributed forces developed during accidents, could explain the common types of mandibular fractures.

## 2. Materials and Methods

CAD software (Solidworks) with reverse engineering capability (ScanTo3D) was used for reconstruction of human mandibular surfaces on the basis of an imported stereolithography triangle surface (STL) file model of the 12 years-old adolescent. Thickness of cortical bone layer was estimated basing on average literature data [47]. Teeth were redesigned because the three-dimensional reconstruction of teeth with periodontal ligament and alveolar socket from medical imaging is cumbersome and specialized software is still under development [48]. Teeth roots were simplified and slightly contracted in radial direction leading to an increase of gap between adjacent teeth in the mandible larger than naturally observed. This modification was necessary to avoid problems in mesh generation due to small gaps between adjacent teeth and chosen mean element size. Concerning the hard tissues of teeth, only dentine was taken into account. Enamel was neglected because of a weak influence of this thin layer on stress field in mandible. The resulting FE mesh (Ansys, Workbench) is illustrated (Fig. 1).

Mesh involved 558838 nodes and 381189 tetrahedral 10-node elements (Ansys, TET10). Statistics of elements' quality is displayed in Fig. 2a. Poor quality elements (having Jacobean lower than 0.25) are highlighted in Fig. 2b. The elastic, linear and isotropic 30 constitutive law was assumed for all involved tissues. The associated mechanical properties are summarized in Table 1

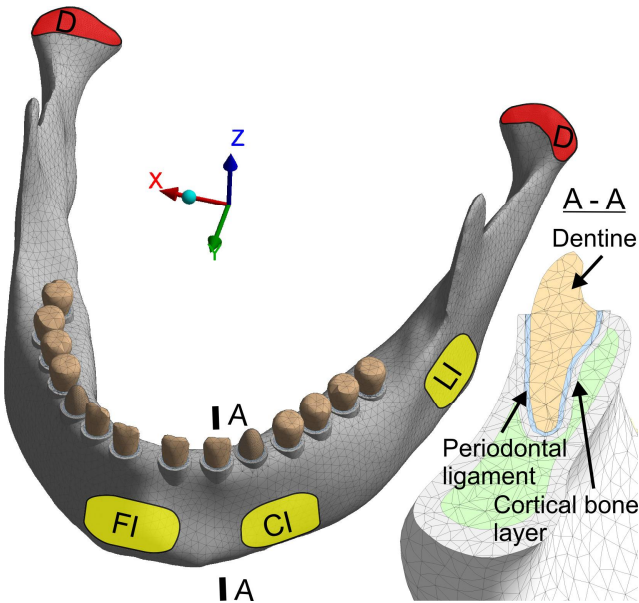


**Figure 1.** Finite element model of the mandible and cross-section view by the incisor tooth with arrangement of tissues in alveolar processes taking into account periodontal ligament in cortical bone socket. The force of 700 N simulating an impact in XY (occlusal) plane was subsequently applied centrally (FI), at canine zone (CI) and at the mandibular angle (LI).

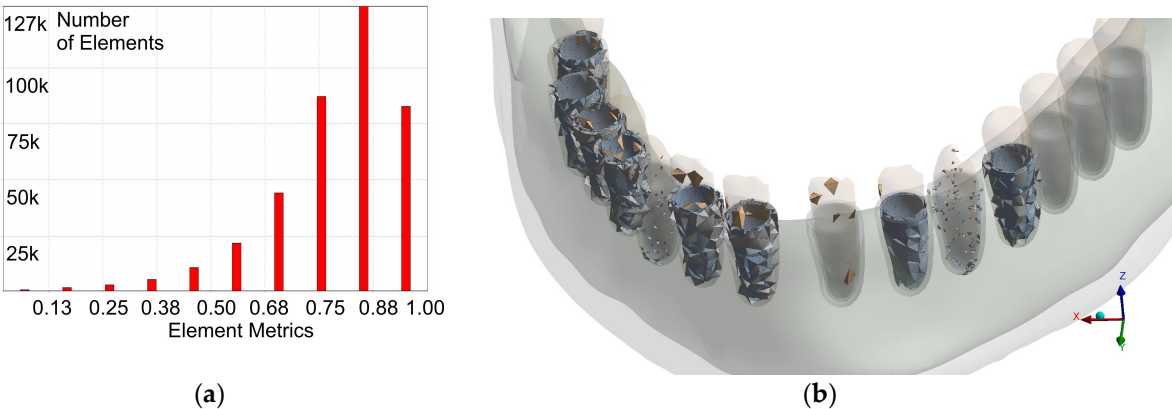


**Figure 2.** Statistics (a) and location (b) of poor quality elements (with quality parameter lower than 0.25).

To simulate impact to the mandible, a distributed horizontal force (parallel to occlusal plane XY) of 700N of magnitude was applied [49]. Three load cases were simulated: Frontal Impact (FI) to the mental protuberance ( $F_Y = -700\text{N}$ ), Impact to Canine (CI) region ( $F_X = -367,73\text{N}$ ;  $F_Y = 595,63\text{N}$ ) and Lateral Impact (LI) to mandibular angle ( $F_X = 700\text{N}$ ). The blow force was distributed on the relatively large areas, illustrated in Figure 1, because the study was not addressed to bone split at the impact-concerned cross-sections of mandible. Fixing the appropriate components of displacement vector on the condylar surfaces in contact with the temporo-mandibular discs (red area named "D" in Figure1) eliminated the rigid body motion of the model.

Fracture risk of the mandible was evaluated using two simple criteria based on the maximal principal stress and maximal principal strain values, well adapted for quasi-elastic materials such as cortical bones. The values used in this paper were deduced from the work of Öhman et al. [50], Reilly and Burstein [51], Martin et al. [52] and Currey and Pond [53]. The retained range of ultimate tensile ( $\sigma_u$ ) stress is  $88 < \sigma_u < 130 \text{ MPa}$ , whereas this of the ultimate tensile strain ( $\epsilon_u$ ) was estimated to be  $0.009 < \epsilon_u < 0.012$ .

**Table 1.** Material properties assumed for the tissue linear behavior.

Material	Young's modulus, MPa	Poisson's ratio
Cortical bone	12 000	0.3
Cancellous bone	800	0.3
Dentine	12 000	0.3
Alveolar cortical bone socket	12 000	0.3
Periodontal ligament	50	0.48

**3. Results**

Figures from 3 to 5 illustrate the obtained results. They show the color-maps of the maximal principal stress and strain for three load-cases studied. The legends of these figures were defined in such manner that the bounds of the red color correspond to the lower and upper bounds of the critical value of the principal stress or strain.

Cortical bone strength has been exceeded in the model of the mandible in all the analyzed load cases. Zones of the potential fracture predominantly depend on the direction of the impact force.

In the case of the quasi-symmetric blow to chin (FI) illustrated in Fig. 3, mainly the neck regions of condylar processes were exposed to fracture due to very intense tension on its upper side. The strain distribution confirms the potential damage zones.

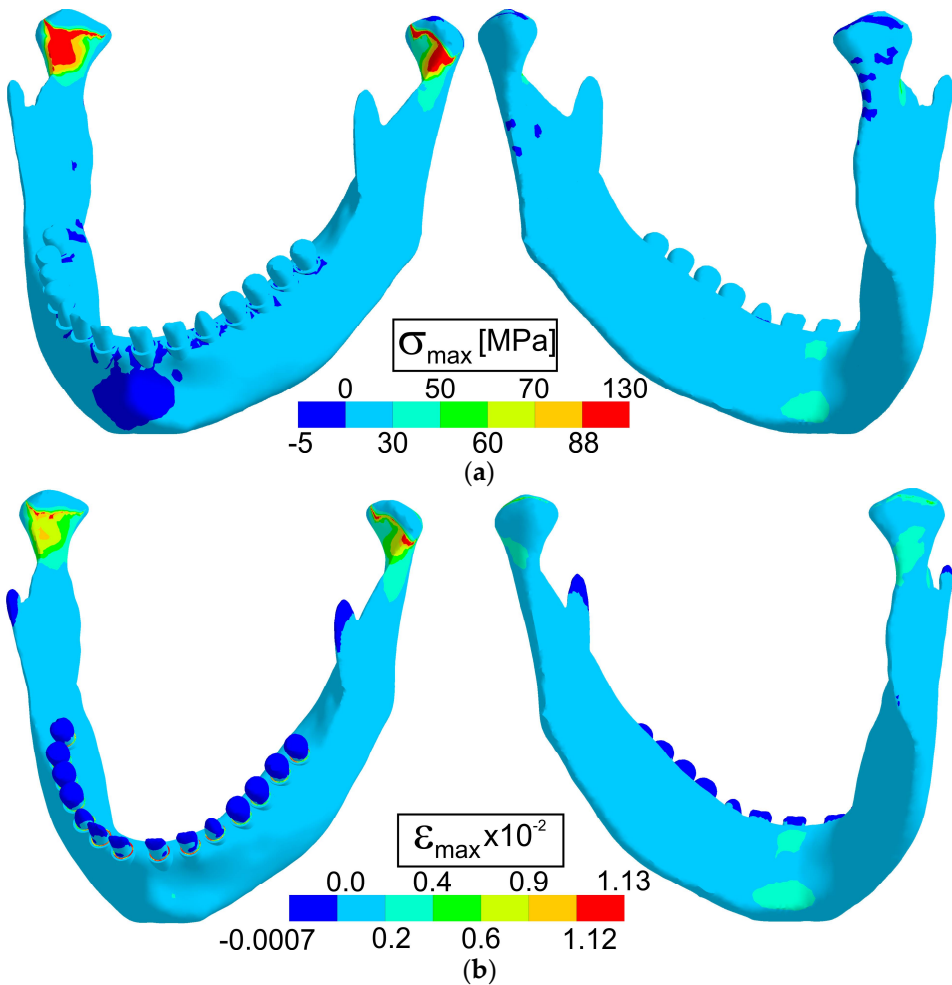


**Figure 3.** Maps of maximal principal stress a) and maximal principal strain b) in the case of quasi-central blow (FI) to anterior region.

Blow to canine region (Fig.4) leads to intense tensile stress in the necks and also at mesial side. The tensile strain exceeded in the left neck (impacted side) its critical value as it can be appreciated in the same figure. Moreover, the critical stress were also surpassed at mesial side of the mandible.

The fracture risk was detected in the mandibular angle due to tensile stress and elevated strain in the case of lateral blow (LI) as it can be appreciated in Fig. 5. Critical tensile stress was exceeded on the lingual surface of the impacted side of mandible. The condylar process at the blown side was more vulnerable to fracture. Also, at the non-blown side the level of tensile stress at the bottom surface of the condylar neck could be considered as dangerous. Elevated tension in parasymphyseal region was detected. The principal strain field confirms these observations.

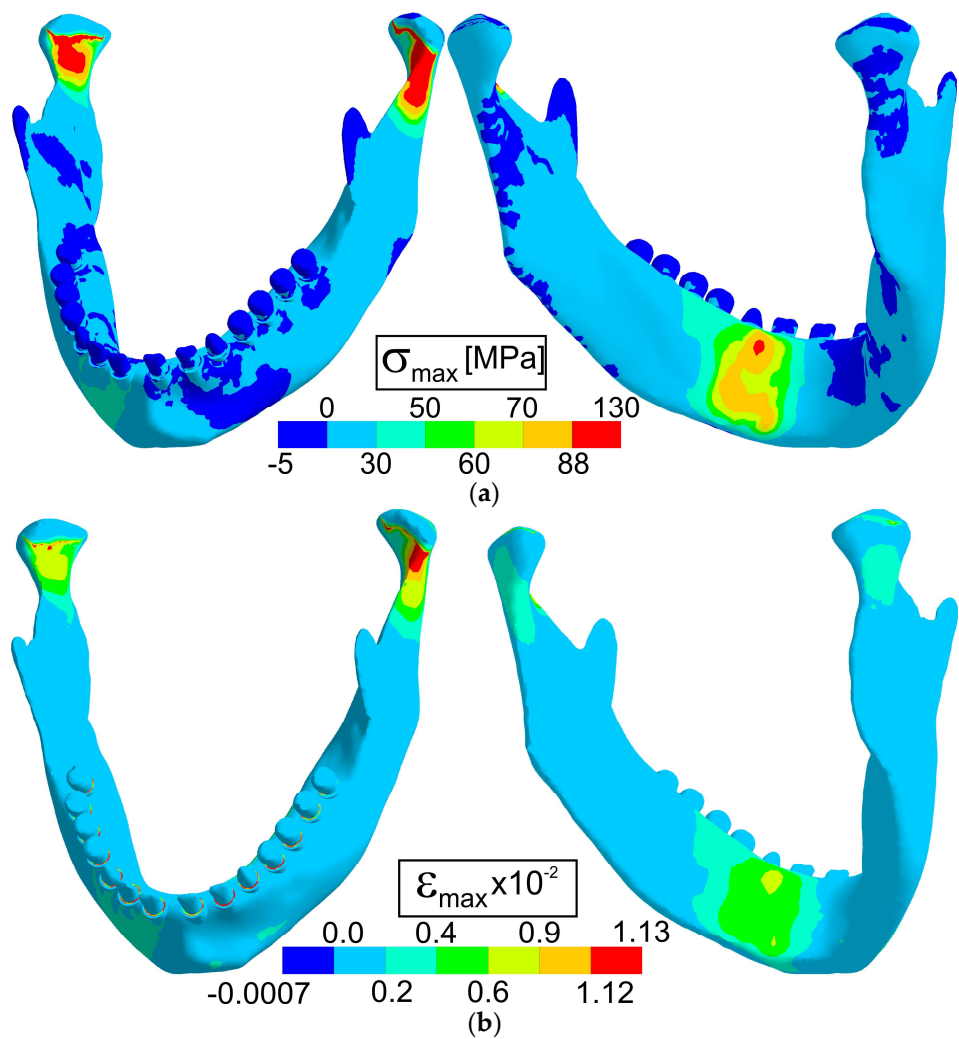


**Figure 4.** Maps of (a) maximal principal stress and (b) maximal principal strain in the case of blow to canine region (CI).



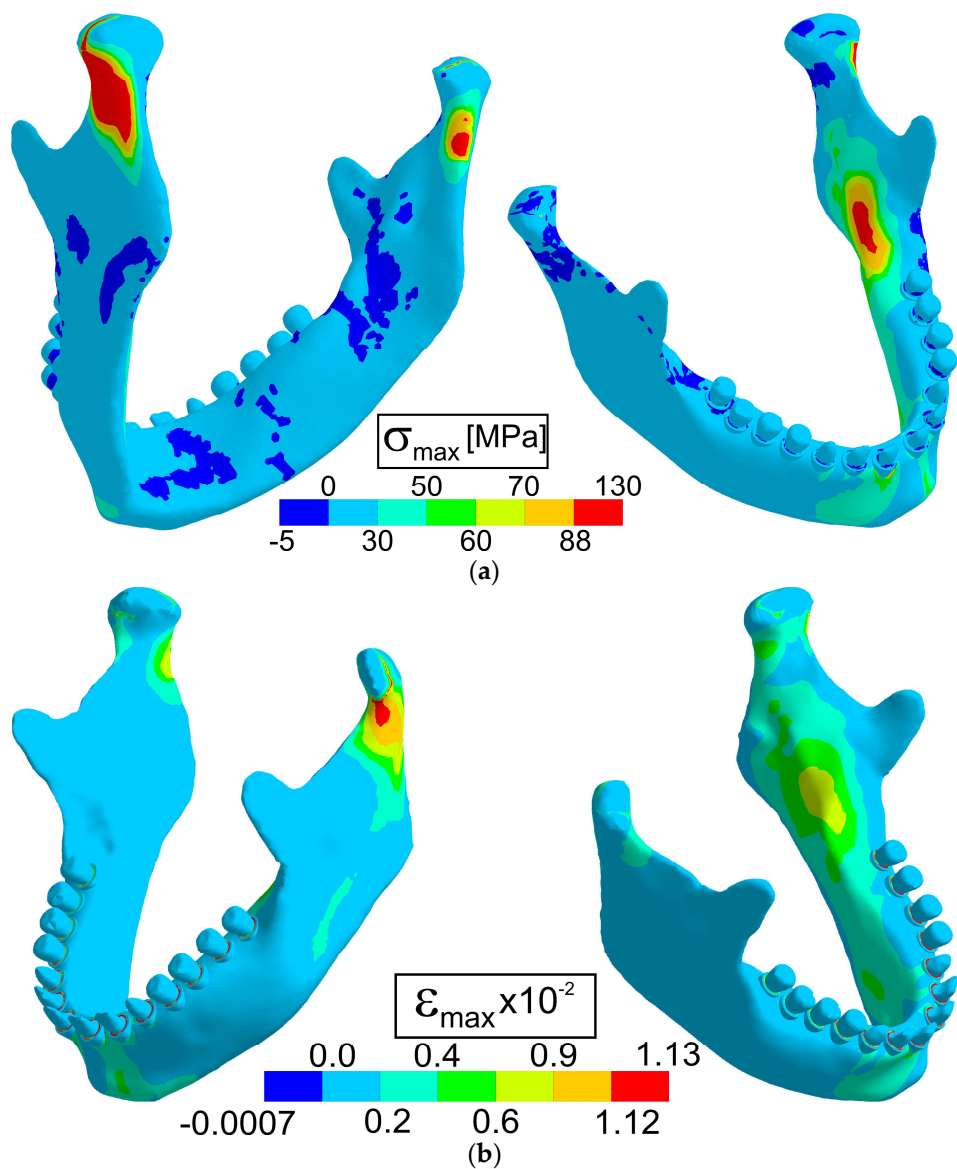


**Figure 5.** Maps of maximal principal stress (a) and maximal principal strain (b) in the case of lateral blow to mandibular angle (LI).

**4. Discussion**

A number of simplifications are being applied in research devoted to simulation of mandible biomechanics. Reasons for this are the high complexity in terms of geometric layouts and tissues' behavior but also in terms of muscle activities and contact interactions generated which depend on the boundary conditions used. In the presented study the average hypothetical dimensions of adolescent mandibular bone with minor geometrical simplifications were assumed. Mesh generation with closely spaced teeth failed or numerous poor quality elements were produced, which introduce difficulties with interpretation of obtained stress and strain fields. To avoid this problem simplification related to local anatomical details such as intervals between teeth were introduced. The intervals broadening can disturb local mechanical fields in some extent, however difficulties associated with finite element mesh generation and poor element quality in the spaces between alveolar processes have been avoided. This problem is well recognized and special algorithms of finite element mesh generation dedicated to mandible with anatomical details of natural dentition are under development [48]. Teeth separation prevents over-stiffening that can affect stress pattern in retromolar region [42] because teeth splinting creates rigid arch. Such artificial "reinforcement" may carry an excessive part of external load inducing an under-loading of alveolar processes.

Hence, stiffness of the mandible model used in this work matches better the actual one when comparing with models where periodontal ligament is directly connected to cancellous bone. Consequently, cancellous tissue around tooth is less stressed during bending and screwing of mandible, because stress is distributed through stiffer cortical sockets onto the exterior and interior parts of the mandibular bone.

The in vitro experimental study of Craig et al. [54] enables the evaluation of the inertia effect during the direct impact of human mandible at the chin area. In the discussion below the test on sample "2329" is analyzed. This test was performed under the following conditions: 2.8 kg mass at drop height of 500 mm. This drop height corresponds to the initial impact velocity of  $VO \approx 3.13 \text{ m/s}$  ( $VO \approx 11.25 \text{ km/h}$ ). The work [54] provides among others the records of displacements of three markers, located at the chin and mandible condyles. The peak impact force of  $\sim 2.300 \text{ N}$  was recorded at time  $\sim 0.01 \text{ s}$ . The displacements were recorded for time span going from 0 to 0.02 s every 1 ms. Knowing the displacement, the velocity and acceleration of the markers can be calculated. Usual discrete approximations of first and second derivatives of displacement were used, namely:

$$v(t_i + \Delta t / 2) = \frac{u(t_{i+1}) - u(t_i)}{\Delta t}, \quad (1)$$

and

$$a(t_i) = \frac{u(t_{i+1}) - 2u(t_i) + u(t_{i-1}))}{(\Delta t)^2}, \quad (2)$$

The plots of Fig. 6 illustrate the velocity profiles.

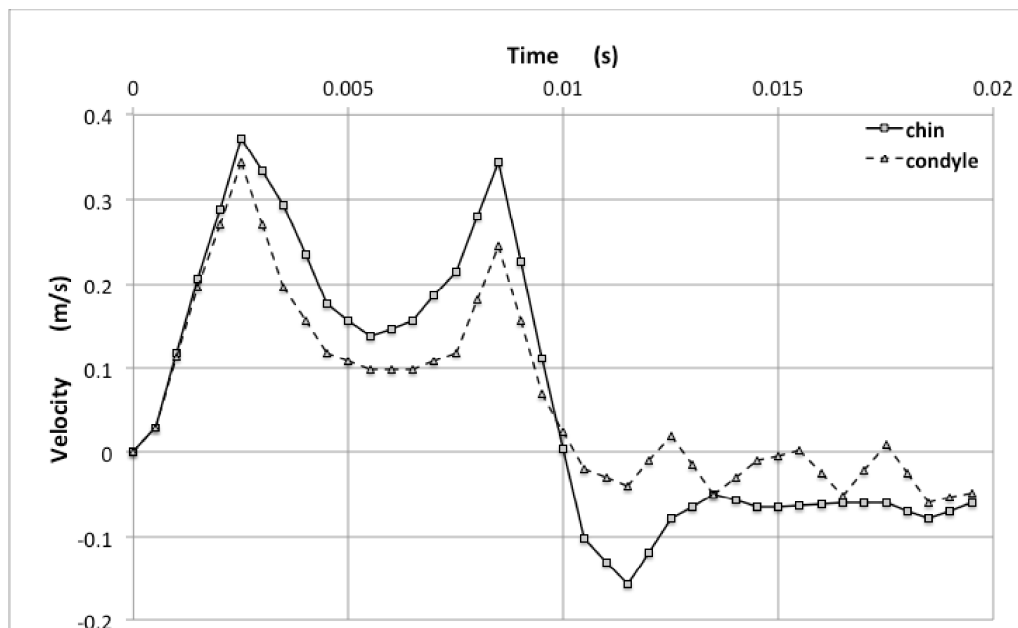


**Figure 6.** Profiles of velocity of markers fixed to the chin and condyles of sample 2329 obtained from the records of their displacements taken from Craig et al. [54]

During the loading phase ( $t < 0.01 \text{ s}$ ) the chin and condyles move in similar manner. The velocity of the condyles' markers being less than that of the chin, the mandible remained in compressive state. Also, the velocity of these points becomes zero at  $t \approx 0.01 \text{ s}$ , the instant for which the impact force becomes maximal. Obviously at that moment the velocity of impacting mass is also nil and its acceleration is maximal. The plots of accelerations of the same markers are presented (Fig. 7). During the loading phase the similar oscillatory behavior of these plots testifies that the mandible vibrated at a frequency of  $f \approx 160 \text{ Hz}$ . Similar frequencies were determined by Craig et al. [54]. The maximal vibration amplitude obtained at  $t \approx 0.01 \text{ s}$  is close to  $200 \text{ m/s}^2$ . If we suppose that the mass associated with this mode of vibration is equal to the total mass of the mandible (exaggerated

estimation), the involved inertial forces can be evaluated. Taking this mass equal to 0.2 kg, the inertia force of 40 N is obtained. This force represents about 1.5% of the peak force of 2300 N recorded during the test. Consequently, the vibration of the mandible can be neglected in analysis of the risk of bone fracture corresponding to the load peak. On the other hand, stress and strain fields can be significantly modulated during the initial loading phase ( $t < 0.003$  s and  $F < 400$  N). Indeed, during this period of loading phase the inertia force represents approximately 10% of the impact force.

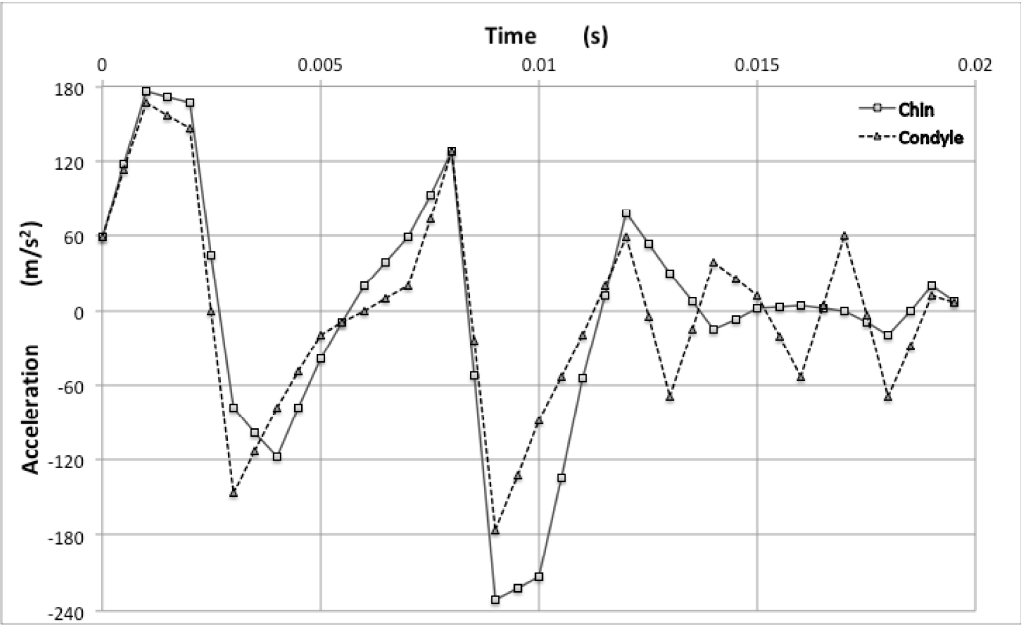


**Figure 7.** Profiles of acceleration of markers fixed to the chin and condyles of sample 2329 obtained from the records of their displacements taken from Craig et al. [54]

It is important to underline that the above evaluation is valid only for initial impact velocities less than 15 km/h. Simple evaluation of kinetic energy of the impacting mass suggests that inertial forces can represent more than 15% of the peak forces for impact velocities greater than 60 km/h.

The fracture tolerance of the mandible revealed experimentally on forty-five cadaver face impacts [49,55] ranged between 685 and 1779 N. Impact investigations showed relatively higher values of tolerance forces reaching 2840 N (Yoganandan et al. [56]) and more than 3000 N [54,57]. So, the value of impact force applied to the mandible in this study corresponded to the lower fracture tolerance of the mandible. It is important to note that in all these experimental studies the mechanical interaction of mandible corresponding to its occlusion state was rarely controlled. It is easy to understand that fracture modes of mandible are strongly depended on contacts of antagonist teeth due to decrease of possible bending and torsion of whole mandible. In case of occlusion, a fracture of condylar necks is possible only during slide of mandible on occluded teeth and condyle bending. Fixation of occlusion with use of silicone [58] results in unknown allowable displacements due to silicone resiliency. On the other hand, in cadaveric study [57], the authors observed that the mandible could move with respect to maxillary despite the occlusion force of 200 N. In the finite element study [37] forces transferred to condyles reached only 60% of the impact force to chin when the model included dentition, however mechanics of occlusion state was not clearly described. In our preliminary study, fracture of stable occluded mandible (rigidly fixed on teeth) appeared only in loaded regions. To avoid this phenomenon, occlusion was renounced in the work. Another factors [59] such as bone and joint irreversible deformation or/and facial, oral and muscle soft tissue damping might influence the mandible fracture.

In real situations, occlusal forces appear as reactions on teeth that are generated due to the muscular activity. Frequently, especially in modeling of occlusion load transfer in mandible, the role of these forces is inverted leading to so called "transposed models"; the reactions are applied as active forces and the muscular actions are deduced as reactions generated at points of the muscular



attachments [13]. To avoid non-physiological behavior of inactive muscles (compressive state of stress), the opening muscles are deactivated or omitted. Such "transposed models" works well during occlusion analysis, however this approach [42] cannot be used to model an external impact on mandible. The behavior of muscular system is very difficult to deduce. Moreover, during blow to disoccluded mandible the closing muscles (elevators) are weakly activated, because of disocclusion state. Hence, weak ability of muscles to resist a blow forces allows neglecting their influence. Also, Lotz and Hayes [60] report that the load absorption during hip fracture is mainly related to soft tissue deformation. However, mandible is coated with a relatively thin soft tissue comparing with the hip, which is protected by thick layer of soft tissues. Consequently, damping ability of facial soft tissues was omitted in the model.

As demonstrated in Bonnet et al. [24], the bone anisotropy plays an important role in stress and strain distribution around the implants. However, in the case of load by external forces the global distribution of stresses is only slightly influenced by the material anisotropy. Consequently, isotropic behavior of all involved tissues was chosen. This simplification allows preventing complicated identification of the orientation of local orthotropic material frames, being frequently subject of controversy.

Statistically, as reported in the work [4], most frequent fractures of mandibles were observed in the condylar region (about 32%), in the symphyseal-parasymphyseal region (29.3%) and in the angular region (20%). The zones of highest stresses and strains in the model coincide with occurrence of these fractures during accidents. Indeed, tension stresses reached the highest level in these regions, except for the symphyseal area under frontal impact. In this region the predicted tension stress and elongations remained relatively moderate, probably due to the uniform distribution of blow force on relatively large area. Perhaps, fractures in this region occur under more concentrated loads during hit in uneven barriers. The high level of fractures in the parasymphyseal region was in agreement with high tension during blow to canine zone. Fracture of tooth and alveolar processes frequently occurs under direct load on tooth or indirect load during contact with opposite tooth. The risk of fracture in dento-alveolar region was not detected, although disocclusion state had been analyzed. In the coronoid and the dento-alveolar regions, the obtained stresses were lower, what is in accordance with only 1.2-1.9% fractures reported by Motamedi [4]. Following the clinical statistics, occurrences of body and ramus fractures are relatively minor; they correspond respectively to 12.5% and 3.1% of mandibular fractures. The details of clinical data concerning the identification of blow location are rarely provided. However, high tension predicted at mesial side can change location due to adequate placing of blow force. When the impact was closer to the parasymphyseal region (CI case), elevated tension was in agreement with frequent fractures [4,61]. The frequent parasymphyseal fractures [4,61] may occur also from arch bending. This sequence of fractures was not simulated but it seems logical that primary condyle fracture and subsequent loss of support at the impacted side, will decrease tension at blown region and increase arch bending. Such a scenario is plausible in view of numerous clinically observed multiple fracture modes (2, 3 or even 4 breaks). Actually, almost half of all mandibular fractures are multiple. Besides, the most frequent among them (24.6%)[61] are angulus-parasymphysis fracture combinations.

The locations of largest stresses were consistent with the results reported in study [39]. However, the authors of this paper assumed very high value of Young's modulus for cancellous bone, quoted 7.93 GPa. Also, the periodontal ligament was not taken into account in their model. The obtained stress values for various blow cases ranged between 162.7 to 808.2 kg/m<sup>2</sup> (1.6-7.9 kPa). The blow force was applied as a pressure of 1.107 Pa. on the area of about 10 mm<sup>2</sup>. It leads to the blow force of approximately 1000 N. In our model stress values were significantly higher and exceeded locally the value of cortical bone strength. The dependence of strength of cortical bone tissue on bone content during growth period is under debate [47,50]. Cortical bone in adolescence is characterized by about 1/3 lower density compared to that of adults. Compression tests [50] performed on adolescent bone tissue showed also that its strength is about 33% lower than for adult tissue, although, ultimate strain was 25% higher in the child. Tensile critical stress was simply

evaluated in our study since the appropriate data (for adolescents) was not found in the open literature. The less stiff bone experiences greater deflection and consequently the fracture energy of specimen is higher [50,62]. In contrast, in the work [47] the same range of ultrasound wave celerity and stiffness were found for children's and elderly adults' bone. Compressive yield strain occurred [50,63] in the range of 0.9-1.3% and it can be taken as invariant with respect to tissue mineral density.

Further studies, on wider group of cases of geometry and density of mandibular bone, are needed to evaluate an impact or influence of the patient specific variables [64]. However, such a study requires medical imaging of a numerous healthy adolescent mandibles and prevalence of special software that will allow easy patient specific three-dimensional tissue reconstruction of alveolar sockets.

Finally, it is important to stress that simulation of impact in a closed or occlusion state, during which the blow force is distributed between TMJs and teeth, does not allow predicting the clinically observed mandible fractures. They are however well reproduced under the assumption of the mandible disocclusion retained in this work. Relationships between TMJ's reactions and occlusal forces during mastication are relatively well understood [13,24,65]. Nonetheless, the role of TMJs during the impact to the mandible is still not clarified. This point and also the question of TMJ disc damage induced by a blow to the mandible needs additional works including disc's tissue regional elasticity [66].

**5. Conclusions**

The location of extreme stresses and strains in the mandible under blow forces, obtained by finite element simulations in linear elastic and static analysis, is in agreement with the most frequent clinical fractures associated with standard accidents. The assumption of disocclusion was necessary to find this agreement. The main conclusion is that smaller force is necessary to fracture disoccluded mandible than occluded one. This point is crucial in fracture prevention and forensic investigations. The strong simplification of interactions in temporo-mandibular joint needs improvements. However, the reliable material data concerning TMJ discs are necessary.

**Funding:** This publication was co-financed by a statutory grant from the Faculty of Mechanical Engineering of the Silesian University of Technology in 2018.

**Conflicts of Interest:** The authors declare no conflict of interest.

**References**

1. Ozawa, T.; Takeda, T.; Ishigami, K.; Narimatsu, K.; Hasegawa, K.; Nakajima, K.; Noh, K. Shock absorption ability of mouthguard against forceful, traumatic mandibular closure. *Dent Traumatol* **2014**, *30*, 204–210, doi:10.1111/edt.12063.
2. Haug, R.H.; Prather, J.; Indresano, A.T. An epidemiologic survey of facial fractures and concomitant injuries. *J. Oral Maxillofac. Surg.* **1990**, *48*, 926–932.
3. Vetter, J.D.; Topazian, R.G.; Goldberg, M.H.; Smith, D.G. Facial fractures occurring in a medium-sized metropolitan area: recent trends. *Int J Oral Maxillofac Surg* **1991**, *20*, 214–216.
4. Motamedi, M.H.K. An assessment of maxillofacial fractures: a 5-year study of 237 patients. *J. Oral Maxillofac. Surg.* **2003**, *61*, 61–64, doi:10.1053/joms.2003.50049.
5. Gutta, R.; Tracy, K.; Johnson, C.; James, L.E.; Krishnan, D.G.; Marciani, R.D. Outcomes of mandible fracture treatment at an academic tertiary hospital: a 5-year analysis. *J. Oral Maxillofac. Surg.* **2014**, *72*, 550–558, doi:10.1016/j.joms.2013.09.005.
6. Murakami, S.; Maeda, Y.; Ghanem, A.; Uchiyama, Y.; Kreiborg, S. Influence of mouthguard on temporomandibular joint. *Scand J Med Sci Sports* **2008**, *18*, 591–595, doi:10.1111/j.1600-0838.2007.00698.x.
7. Fahlstedt, M.; Halldin, P.; Kleiven, S. The protective effect of a helmet in three bicycle accidents--A finite element study. *Accid Anal Prev* **2016**, *91*, 135–143, doi:10.1016/j.aap.2016.02.025.

- 321 8. Miralbes, R. Design of motorcycle rider protection systems using numerical techniques. *Accid Anal Prev*  
322 **2013**, *59*, 94–108, doi:10.1016/j.aap.2013.04.016.
- 323 9. Bailly, N.; Llari, M.; Donnadieu, T.; Masson, C.; Arnoux, P.J. Head impact in a snowboarding accident.  
324 *Scand J Med Sci Sports* **2017**, *27*, 964–974, doi:10.1111/sms.12699.
- 325 10. Lloyd, J.D.; Nakamura, W.S.; Maeda, Y.; Takeda, T.; Leesungbok, R.; Lazarchik, D.; Dorney, B.; Gonda, T.;  
326 Nakajima, K.; Yasui, T.; Iwata, Y.; Suzuki, H.; Tsukimura, N.; Churei, H.; Kwon, K.-R.; Choy, M.M.H.;  
327 Rock, J.B. Mouthguards and their use in sports: Report of the 1st International Sports Dentistry Workshop,  
328 2016. *Dent Traumatol* **2017**, *33*, 421–426, doi:10.1111/edt.12375.
- 329 11. Takeda, T.; Ishigami, K.; Nakajima, K.; Naitoh, K.; Kurokawa, K.; Handa, J.; Shomura, M.; Regner, C.W.  
330 Are all mouthguards the same and safe to use? Part 2. The influence of anterior occlusion against a direct  
331 impact on maxillary incisors. *Dent Traumatol* **2008**, *24*, 360–365, doi:10.1111/j.1600-9657.2008.00576.x.
- 332 12. Handa, J.; Takeda, T.; Kurokawa, K.; Ozawa, T.; Nakajima, K.; Ishigami, K. Influence of pre-laminated  
333 material on shock absorption ability in specially designed mouthguard with hard insert and space. *J*  
334 *Prosthodont Res* **2011**, *55*, 214–220, doi:10.1016/j.jpor.2011.02.003.
- 335 13. Chladek, W.; Żmudzki, J.; Lipski, T. Finite element analysis of mandible equilibrium depending on the  
336 way of its loading and supporting. *Acta of Bioengineering and Biomechanics* **2000**, Vol. 2, 63–69.
- 337 14. Tanaka, E.; Hirose, M.; Inubushi, T.; Koolstra, J.H.; van Eijden, T.M.G.J.; Suekawa, Y.; Fujita, R.; Tanaka,  
338 M.; Tanne, K. Effect of hyperactivity of the lateral pterygoid muscle on the temporomandibular joint disk.  
339 *J Biomech Eng* **2007**, *129*, 890–897, doi:10.1115/1.2800825.
- 340 15. Pérez del Palomar, A.; Doblaré, M. Influence of unilateral disc displacement on the stress response of the  
341 temporomandibular joint discs during opening and mastication. *J. Anat.* **2007**, *211*, 453–463,  
342 doi:10.1111/j.1469-7580.2007.00796.x.
- 343 16. Creuillot, V.; Areiza, D.A.; de Brosses, E.S.; Bonnet, A.S.; Lipinski, P. Finite element analysis of  
344 temporomandibular joints during opening-closing motion: asynchronous case report. *Comput Methods*  
345 *Biomech Biomed Engin* **2013**, *16 Suppl 1*, 300–301, doi:10.1080/10255842.2013.815910.
- 346 17. Lovald, S.T.; Wagner, J.D.; Baack, B. Biomechanical optimization of bone plates used in rigid fixation of  
347 mandibular fractures. *J. Oral Maxillofac. Surg.* **2009**, *67*, 973–985, doi:10.1016/j.joms.2008.12.032.
- 348 18. Kromka-Szydek, M.; Jedrusik-Pawłowska, M.; Milewski, G.; Lekston, Z.; Cieślík, T.; Drugacz, J. Numerical  
349 analysis of displacements of mandible bone parts using various elements for fixation of subcondylar  
350 fractures. *Acta Bioeng Biomech* **2010**, *12*, 11–18.
- 351 19. Jedrusik-Pawłowska, M.; Kromka-Szydek, M.; Katra, M.; Niedzielska, I. Mandibular  
352 reconstruction--biomechanical strength analysis (FEM) based on a retrospective clinical analysis of  
353 selected patients. *Acta Bioeng Biomech* **2013**, *15*, 23–31.
- 354 20. Boccaccio, A.; Pappalettere, C.; Kelly, D.J. The influence of expansion rates on mandibular distraction  
355 osteogenesis: a computational analysis. *Ann Biomed Eng* **2007**, *35*, 1940–1960,  
356 doi:10.1007/s10439-007-9367-x.
- 357 21. Bonnet, A.-S.; Dubois, G.; Lipinski, P.; Schouman, T. In vivo study of human mandibular distraction  
358 osteogenesis. Part II: Determination of callus mechanical properties. *Acta Bioeng Biomech* **2013**, *15*, 11–18.
- 359 22. Dejak, B.; Młotkowski, A. 3D-Finite element analysis of molars restored with endocrowns and posts  
360 during masticatory simulation. *Dent Mater* **2013**, *29*, e309–317, doi:10.1016/j.dental.2013.09.014.
- 361 23. Żmudzki, J.; Chladek, G.; Kasperski, J. Biomechanical factors related to occlusal load transfer in removable  
362 complete dentures. *Biomech Model Mechanobiol* **2015**, *14*, 679–691, doi:10.1007/s10237-014-0642-0.

24. Bonnet, A.S.; Postaire, M.; Lipinski, P. Biomechanical study of mandible bone supporting a four-implant retained bridge: finite element analysis of the influence of bone anisotropy and foodstuff position. *Med Eng Phys* **2009**, *31*, 806–815, doi:10.1016/j.medengphy.2009.03.004.
25. Żmudzki, J.; Chladek, G.; Kasperski, J.; Dobrzański, L.A. One versus two implant-retained dentures: comparing biomechanics under oblique mastication forces. *J Biomech Eng* **2013**, *135*, 54503, doi:10.1115/1.4023985.
26. Zmudzki, J.; Chladek, G.; Kasperski, J. Single implant-retained dentures: loading of various attachment types under oblique occlusal forces. *J. Mech. Med. Biol.* **2012**, *12*, 1250087, doi:10.1142/S021951941250087X.
27. Zmudzki, J.; Chladek, W.; Lipski, T. Influence of tongue activity on lower complete denture retention under biting forces. *Acta Bioeng Biomech* **2008**, *10*, 13–20.
28. Żmudzki, J.; Chladek, G.; Krawczyk, C. Relevance of Tongue Force on Mandibular Denture Stabilization during Mastication. *J Prosthodont* **2017**, doi:10.1111/jopr.12719.
29. Meng, Y.; Pak, W.; Guleyupoglu, B.; Koya, B.; Gayzik, F.S.; Untaroiu, C.D. A finite element model of a six-year-old child for simulating pedestrian accidents. *Accid Anal Prev* **2017**, *98*, 206–213, doi:10.1016/j.aap.2016.10.002.
30. Dawson, J.M.; Khmelniker, B.V.; McAndrew, M.P. Analysis of the structural behavior of the pelvis during lateral impact using the finite element method. *Accid Anal Prev* **1999**, *31*, 109–119.
31. Tse, K.M.; Tan, L.B.; Lee, S.J.; Lim, S.P.; Lee, H.P. Investigation of the relationship between facial injuries and traumatic brain injuries using a realistic subject-specific finite element head model. *Accid Anal Prev* **2015**, *79*, 13–32, doi:10.1016/j.aap.2015.03.012.
32. Shaoo, D.; Deck, C.; Yoganandan, N.; Willinger, R. Influence of stiffness and shape of contact surface on skull fractures and biomechanical metrics of the human head of different population under lateral impacts. *Accid Anal Prev* **2015**, *80*, 97–105, doi:10.1016/j.aap.2015.04.004.
33. Ruan, J.; Prasad, P. The effects of skull thickness variations on human head dynamic impact responses. *Stapp Car Crash J* **2001**, *45*, 395–414.
34. Yoganandan, N.; Pintar, F.A. Biomechanics of temporo-parietal skull fracture. *Clin Biomech (Bristol, Avon)* **2004**, *19*, 225–239, doi:10.1016/j.clinbiomech.2003.12.014.
35. Bass, C.R.; Yoganandan, N. Skull and Facial Bone Injury Biomechanics. In *Accidental Injury: Biomechanics and Prevention*; Yoganandan, N., Nahum, A.M., Melvin, J.W., Eds.; Springer New York: New York, NY, 2015; pp. 203–220 ISBN 978-1-4939-1732-7.
36. Pajic, S.S.; Antic, S.; Vukicevic, A.M.; Djordjevic, N.; Jovicic, G.; Savic, Z.; Saveljic, I.; Janović, A.; Pesic, Z.; Djuric, M.; Filipovic, N. Trauma of the Frontal Region Is Influenced by the Volume of Frontal Sinuses. A Finite Element Study. *Front Physiol* **2017**, *8*, 493, doi:10.3389/fphys.2017.00493.
37. Tuchtan, L.; Piercecchi-Marti, M.-D.; Bartoli, C.; Boisclair, D.; Adalian, P.; Léonetti, G.; Behr, M.; Thollon, L. Forces transmission to the skull in case of mandibular impact. *Forensic Sci. Int.* **2015**, *252*, 22–28, doi:10.1016/j.forsciint.2015.04.017.
38. Lin, S.-L.; Lee, S.-Y.; Lee, L.-Y.; Chiu, W.-T.; Lin, C.-T.; Huang, H.-M. Vibrational analysis of mandible trauma: experimental and numerical approaches. *Med Biol Eng Comput* **2006**, *44*, 785–792, doi:10.1007/s11517-006-0095-4.
39. Gallas Torreira, M.; Fernandez, J.R. A three-dimensional computer model of the human mandible in two simulated standard trauma situations. *J Craniomaxillofac Surg* **2004**, *32*, 303–307, doi:10.1016/j.jcms.2004.04.008.

40. Santos, L.S. de M.; Rossi, A.C.; Freire, A.R.; Matoso, R.I.; Caria, P.H.F.; Prado, F.B. Finite-element analysis of 3 situations of trauma in the human edentulous mandible. *J. Oral Maxillofac. Surg.* **2015**, *73*, 683–691, doi:10.1016/j.joms.2014.10.014.
41. Gröning, F.; Fagan, M.J.; O'Higgins, P. The effects of the periodontal ligament on mandibular stiffness: a study combining finite element analysis and geometric morphometrics. *J Biomech* **2011**, *44*, 1304–1312, doi:10.1016/j.jbiomech.2011.01.008.
42. Bezerra, T.P.; Silva Junior, F.I.; Scarparo, H.C.; Costa, F.W.G.; Studart-Soares, E.C. Do erupted third molars weaken the mandibular angle after trauma to the chin region? A 3D finite element study. *Int J Oral Maxillofac Surg* **2013**, *42*, 474–480, doi:10.1016/j.ijom.2012.10.009.
43. Bezerra, T.-P.; Studart-Soares, E.-C.; Pita-Neto, I.-C.; Costa, F.-W.-G.; Batista, S.-H.-B. Do third molars weaken the mandibular angle? *Med Oral Patol Oral Cir Bucal* **2011**, *16*, e657-663.
44. Żmudzki, J.; Walke, W.; Chladek, W. Influence of Model Discretization Density in FEM Numerical Analysis on the Determined Stress Level in Bone Surrounding Dental Implants. In *Information Technologies in Biomedicine*; Pietka, E., Kawa, J., Eds.; Advances in Soft Computing; Springer Berlin Heidelberg, 2008; pp. 559–567.
45. Biały, M.; Stankiewicz, M.; Stempniewicz, A.; Cymer-Biała, M.; Minch, L. Dentists' Attitudes Towards Mouthguards Used by Young Athletically-Active Patients. *Dental and Medical Problems* **2014**, *51*, 382–386.
46. Fakhruddin, K.S.; Lawrence, H.P.; Kenny, D.J.; Locker, D. Use of mouthguards among 12- to 14-year-old Ontario schoolchildren. *J Can Dent Assoc* **2007**, *73*, 505.
47. Berteau, J.-P.; Baron, C.; Pithioux, M.; Launay, F.; Chabrand, P.; Lasaygues, P. In vitro ultrasonic and mechanic characterization of the modulus of elasticity of children cortical bone. *Ultrasonics* **2014**, *54*, 1270–1276, doi:10.1016/j.ultras.2013.09.014.
48. Ding, X.; Liao, S.-H.; Zhu, X.-H.; Wang, H.-M. Influence of orthotropy on biomechanics of peri-implant bone in complete mandible model with full dentition. *Biomed Res Int* **2014**, *2014*, 709398, doi:10.1155/2014/709398.
49. Hampson, D. Facial injury: a review of biomechanical studies and test procedures for facial injury assessment. *J Biomech* **1995**, *28*, 1–7.
50. Öhman, C.; Baleani, M.; Pani, C.; Taddei, F.; Alberghini, M.; Viceconti, M.; Manfrini, M. Compressive behaviour of child and adult cortical bone. *Bone* **2011**, *49*, 769–776, doi:10.1016/j.bone.2011.06.035.
51. Reilly, D.T.; Burstein, A.H. The elastic and ultimate properties of compact bone tissue. *J Biomech* **1975**, *8*, 393–405.
52. Martin, R.B.; Burr, D.B.; Sharkey, N.A. Mechanical Properties of Bone. In *Skeletal Tissue Mechanics*; Martin, R.B., Burr, D.B., Sharkey, N.A., Eds.; Springer New York: New York, NY, 1998; pp. 127–180 ISBN 978-1-4757-2968-9.
53. Currey, J.D.; Pond, C.M. Mechanical properties of very young bone in the axis deer (*Axis axis*) and humans. *Journal of Zoology* **1989**, *218*, 59–67, doi:10.1111/j.1469-7998.1989.tb02525.x.
54. Craig, M.; Bir, C.; Viano, D.; Tashman, S. Biomechanical response of the human mandible to impacts of the chin. *J Biomech* **2008**, *41*, 2972–2980, doi:10.1016/j.jbiomech.2008.07.020.
55. Nyquist, G.W.; Cavanaugh, J.M.; Goldberg, S.J.; King, A.I. Facial Impact Tolerance and Response. *SAE Transactions* **1986**, *95*, 850–871.
56. *Accidental Injury: Biomechanics and Prevention*; Yoganandan, N., Nahum, A.M., Melvin, J.W., Eds.; 3rd ed.; Springer-Verlag: New York, 2015; ISBN 978-1-4939-1731-0.



57. Unnewehr, M.; Homann, C.; Schmidt, P.F.; Sotony, P.; Fischer, G.; Brinkmann, B.; Bajanowski, T.; DuChesne, A. Fracture properties of the human mandible. *Int. J. Legal Med.* **2003**, *117*, 326–330, doi:10.1007/s00414-003-0391-6.
58. Hodgson, V.R. Head Model for Impact Tolerance. In *Human Impact Response: Measurement and Simulation*; King, W.F., Mertz, H.J., Eds.; Springer US: Boston, MA, 1973; pp. 113–128 ISBN 978-1-4757-1502-6.
59. Hodgson, V.R. Tolerance of the facial bones to impact. *American Journal of Anatomy* **1967**, *120*, 113–122, doi:10.1002/aja.1001200109.
60. Lotz, J.C.; Hayes, W.C. The use of quantitative computed tomography to estimate risk of fracture of the hip from falls. *J Bone Joint Surg Am* **1990**, *72*, 689–700.
61. Oruç, M.; Işık, V.M.; Kankaya, Y.; Gürsoy, K.; Sungur, N.; Aslan, G.; Koçer, U. Analysis of Fractured Mandible Over Two Decades. *J Craniofac Surg* **2016**, *27*, 1457–1461, doi:10.1097/SCS.00000000000002737.
62. Currey, J.D.; Butler, G. The mechanical properties of bone tissue in children. *J Bone Joint Surg Am* **1975**, *57*, 810–814.
63. Bayraktar, H.H.; Keaveny, T.M. Mechanisms of uniformity of yield strains for trabecular bone. *J Biomech* **2004**, *37*, 1671–1678, doi:10.1016/j.jbiomech.2004.02.045.
64. Hannam, A.G. Current computational modelling trends in craniomandibular biomechanics and their clinical implications. *J Oral Rehabil* **2011**, *38*, 217–234, doi:10.1111/j.1365-2842.2010.02149.x.
65. Abe, M.; Medina-Martinez, R.U.; Itoh, K.; Kohno, S. Temporomandibular joint loading generated during bilateral static bites at molars and premolars. *Med Biol Eng Comput* **2006**, *44*, 1017–1030, doi:10.1007/s11517-006-0075-8.
66. Tappert, L.K.; Baldit, A.; Rahouadj, R.; Lipinski, P. Local elastic properties characterization of the temporo-mandibular joint disc through macro-indentation. *Comput Methods Biomech Biomed Engin* **2017**, *20*, 201–202, doi:10.1080/10255842.2017.1382932.